



# The long-term and far-reaching impact of hurricane Dorian (2019) on the Gulf Stream and the coast



Tal Ezer

Center for Coastal Physical Oceanography, Old Dominion University, 4111 Monarch Way, Norfolk, VA 23508, USA

## ARTICLE INFO

### Keywords:

Coastal sea level  
Hurricanes  
Flooding  
Gulf Stream  
Florida current

## ABSTRACT

Hurricane Dorian (28-August to 6-September 2019) was one of the most powerful hurricanes ever recorded in the Atlantic Ocean; it had disastrous impact on the Bahamas, before moving along the southeastern coast of the U.S. The unusual track of Dorian followed the track of hurricane Matthew (2016)- both hurricanes moved along the Gulf Stream (GS) without making a significant landfall and both seemed to weaken the flow of the GS by almost 50%. In the case of Dorian, the transport of the Florida Current (FC) measured by the cable across the Florida Straits had dropped from 34.7 Sv (1 Sv =  $10^6$  m<sup>3</sup>/s) on 22-August before the storm, to 17.1 Sv on 4-September (the lowest recorded value since measurements started in 1982). Two questions that this study tried to answer are: 1. Did the disruption that Dorian caused to ocean currents off the Florida coast affect the large-scale Gulf Stream (GS) dynamics downstream? and 2. Was there a long-term impact on the GS flow and on coastal sea level? Satellite altimeter data showed that the signal of the hurricane's impact on reducing the GS flow near the Florida coast is seen as far as 4000 km downstream along the GS path 50 days later. This long period of a weakened GS flow can elevate coastal sea level and increase flooding in the days and weeks after offshore storms already disappeared. The observed FC transport was found to be significantly correlated with the downstream GS velocity as far as 50°W and was anti-correlated with sea level along the entire U.S. East Coast. The density and velocity anomaly created by the hurricane's cooling and mixing near the Florida coast seemed to propagate downstream with the GS flow at ~1 m/s, but slow-moving baroclinic waves with propagation speed of ~0.1 m/s were also observed along the GS path. The results of this study may have implications for the indirect impact of storms on large-scale ocean circulation, coastal processes and the response of coastal ecosystems to offshore changes.

## Regional index terms

USA  
East Coast  
Mid-Atlantic Bight  
South Atlantic Bight

## 1. Introduction

Hurricane Dorian was one of the most powerful hurricanes ever recorded in the Atlantic Ocean, reaching category 5 and maximum winds of ~295 km/h (~82 m/s) and central low pressure of 910 mbar. It became a hurricane on August 28th, 2019 and made landfall in the Bahamas on September 1 with disastrous results (Zegarra et al., 2020). After stalling for a couple of days, it moved on September 3 toward the U.S. coast and followed the coast without making significant landfall until moving away toward the open Atlantic Ocean and Canada on 6-

September. The track of this hurricane was quite unusual as the hurricane stalled near the Bahamas for a relatively long time and then followed the path of the Gulf Stream (GS) along the southeastern coast without making significant landfall. The track of Dorian was similar to the track of hurricane Matthew (2016). Matthew was the subject of recent studies that found that the hurricane significantly disrupted the flow of the GS, weakening its flow by almost 50% (Ezer et al., 2017; Ezer, 2018a, 2019a). Measurements of the Florida Current (FC) by the cable across the Florida Straits (Baringer and Larsen, 2001; Meinen et al., 2010) show that during the passage of Dorian the FC transport dropped by ~50% (like during Matthew in 2016) from 34.7 Sv (1 Sv =  $10^6$  m<sup>3</sup>/s) on 22-August before the storm, to 17.1 Sv on 4-September. FC transport of 17.1 Sv was the lowest recorded value since measurements started in 1982 (the second lowest value, 17.2 Sv was during superstorm Sandy in 2012). Observations from gliders also found weakening of the GS by ~40% following hurricanes Irma, Jose, and Maria in 2017 (Todd et al., 2018). In fact, one can find reduced FC

E-mail address: [tezer@odu.edu](mailto:tezer@odu.edu).

<https://doi.org/10.1016/j.jmarsys.2020.103370>

Received 2 January 2020; Received in revised form 30 April 2020; Accepted 2 May 2020

Available online 08 May 2020

0924-7963/ © 2020 Elsevier B.V. All rights reserved.

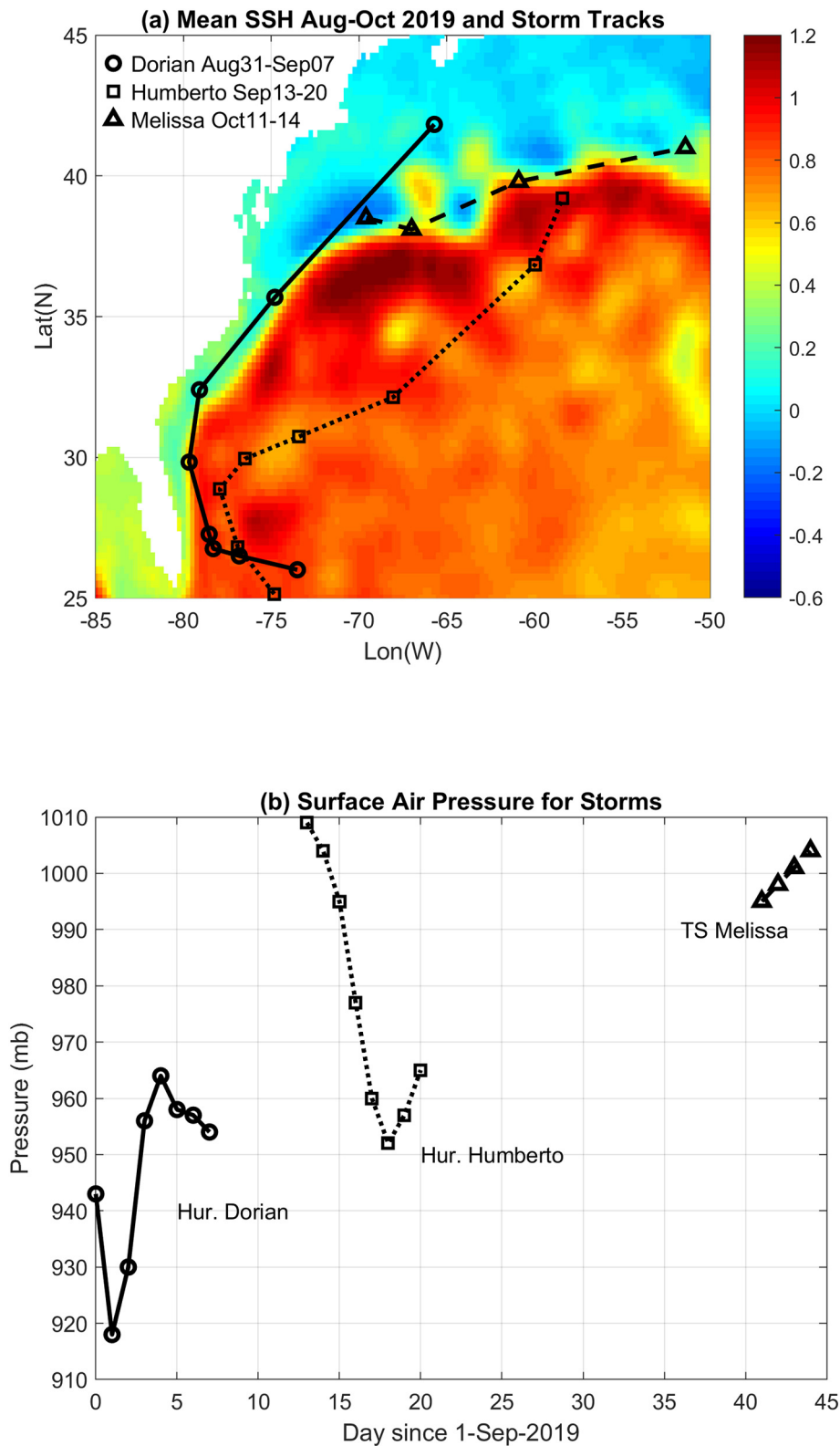


**Fig. 1.** (a) Mean sea surface height (SSH) for August–October 2019 from altimeter data (m, in colour) and the daily track of the three storms discussed in the text. (b) The daily surface minimum air pressure for the three storms. Circles, squares and triangles represent hurricanes Dorian and Humberto and tropical storm Melissa, respectively.

flows for numerous hurricanes that passed close enough to the GS, including Barry (1983), Wilma (2005), Sandy (2012), Joaquin (2015), Matthew (2016), Maria (2017), Florence (2018) and Dorian (2019) (see Fig. 8 in Ezer, 2018b). In those cases, the impact of the hurricanes

lasted from a few days to a few weeks. If the GS remained weaker than normal during this time coastal sea level is higher than normal, causing minor tidal flooding in the days after storms. The numerical simulations of Ezer (2019a) suggest that the impact of hurricanes on the GS can last

for up to 60 days- the slow recovery of the GS is due to the time needed for new warm waters to be advected downstream, replacing the cold waters in the wake of the storm and reestablishing the thermal gradients across the GS front. The large density gradient across the GS front is responsible for the baroclinic geostrophic portion of the GS flow. Tropical cyclones such as hurricanes extract heat from the ocean's surface and mix cooler deep waters with the warmer surface waters; these processes are well documented (Bender and Ginis, 2000; Shay et al., 2000; Li et al., 2002; Oey et al., 2006, 2007; Yablonsky et al., 2015), however, how hurricanes impact ocean circulation is a complex process that not yet fully understood. Some examples of tropical cyclones impacting ocean circulation patterns are seen in numerical simulations of the Gulf of Mexico (Oey et al., 2006, 2007) the North Atlantic (Kourafalou et al., 2016), the GS (Ezer et al., 2017; Ezer, 2018a, 2019a), and even the Kuroshio in the Pacific Ocean Wu et al., 2008; Liu and Wei, 2015).

The impact of tropical cyclones on ocean circulation may have implications for coastal populations and even for coastal ecosystems, where for example, warm GS waters and eddies can intrude into shelf regions (Gawarkiewicz et al., 2012; Hoarfrost et al., 2019). Sea level rise also causes saltwater intrusion into marshlands with ecosystem implications (e.g., Neubauer et al., 2019; Tully et al., 2019). Acceleration of sea level rise along the U.S. East Coast is a major concern (Boon, 2012; Sallenger et al., 2012; Ezer and Corlett, 2012; Ezer, 2013, 2015, 2018b; Park and Sweet, 2015) and there is growing evidence that variations in offshore ocean dynamics and the GS in particular can contribute to variations in coastal sea level (Ezer et al., 2013; Goddard et al., 2015; Wdowinski et al., 2016). The connection between coastal sea level variability and variations in the GS flow is explained by the fact that changes in sea level slope across the GS are proportional to the GS flow intensity (i.e., the geostrophic balance). So, in general, weakening of the GS will raise water on the shoreside of the GS and lower water on the open ocean side of the GS. This idea has been confirmed by satellite data (Ezer et al., 2013) and models (Ezer, 2016) and seems to work on a wide range of time scales from daily variations to decadal and longer (Ezer, 2015). Offshore large-scale signals are transferred into the coast by barotropic open ocean waves and spread along the coast by coastal trapped waves (Huthnance, 1978), resulting in coherent sea level anomalies along long stretches of coasts (Hughes and Meredith, 2006; Thompson and Mitchum, 2014). While statistically significant anti-correlations between the GS flow strength and coastal sea level variability are often found, it does not necessarily indicate a cause and effect and does not exclude other forcing mechanisms. Typical GS to coastal sea level correlation coefficients are around  $-0.4$  to  $-0.5$  for high-frequency oscillations (Ezer, 2016; Ezer and Atkinson, 2017) and around  $-0.8$  for decadal variations (Ezer et al., 2013; Ezer, 2019c), so that GS variability may be responsible to anywhere between 15% and 60% of the coastal variability, depending on the situation and time scale. Contribution from other forcing such as wind and atmospheric pressure can be important to sea level variability (Piecuch et al., 2016; Woodworth et al., 2016), especially in hurricanes with their extreme low surface pressure.

Following on the footsteps of our previous studies of the impact of hurricane Matthew (Ezer et al., 2017; Ezer, 2018a, 2019a), hurricane Dorian with its unprecedented impact on the FC provides an excellent case study to further investigate the extent in time and space of this impact and consequences for the coast. In particular, the study addresses the issue of how local anomalies created by storms at one location are remotely spread farther away from the storm along the coast and along the path of the GS. The study focused on the period August to October 2019, when in addition to Dorian, two other storms passed close to the GS, Hurricane Humberto in September and tropical storm Melissa in October (Fig. 1a), though these two storms were much weaker than Dorian, as seen in their surface pressure (Fig. 1b).

The study is organized as follows. The data sources and the analysis approach are described in section 2, then in section 3 results are

presented for the impact of the storm on the coast and on the Gulf Stream, and finally a summary and conclusions are offered in section 4.

## 2. Data sources and analysis approach

Hourly water level data for Norfolk were obtained from the tide gauge station at Sewells Point (76.33°W, 36.95°N); these data are available from NOAA (<http://opendap.co-ops.nos.noaa.gov/dods/>). Sea surface temperature (SST) images from satellite data were obtained from NOAA/NESDIS (<https://www.nesdis.noaa.gov/>). Daily transport data of the Florida Current (FC) from the cable across the Florida Strait (Baringer et al. 2001; Meinen et al., 2010) were obtained from NOAA/AOML (<http://www.aoml.noaa.gov/phod/floridacurrent/>). Satellite altimeter data were extracted for the North Atlantic Ocean from AVISO (<http://las.aviso.oceanobs.com/las/>); note that these data are also available from the Copernicus site (<http://marine.copernicus.eu/>). The gridded daily composite altimeter data on  $\frac{1}{4}$  degree grid for August to October 2019, include absolute Sea Surface Height (SSH) and SSH anomaly. The absolute SSH( $x,y,t$ ) is the time-averaged mean SSH<sup>avr</sup>( $x,y$ ) plus the anomaly SSH<sup>ano</sup>( $x,y,t$ ) and is relative to the global mean value. The AVISO data also provides gridded surface geostrophic velocity ( $u$  and  $v$  components are calculated from the SSH gradients in the  $y$  and  $x$  directions, respectively). Maximum velocity speed was used to detect the daily track of the GS from the Florida Strait (around 80°W, 27°N) to the GS extension (around 50°W, 40°N); GS rings were removed by detecting abnormal abrupt changes in the track that were clearly not GS meanders. Surface currents near the eye of hurricane Dorian were obtained from the NOAA's operational coupled hurricane-ocean model HWRF-POM ([http://www.emc.ncep.noaa.gov/gc\\_wmb/vxt/HWRF/](http://www.emc.ncep.noaa.gov/gc_wmb/vxt/HWRF/)). The Hurricane Weather Research and Forecasting (HWRF) model was coupled with an ocean model that was evolved from the Princeton Ocean Model (POM; Blumberg and Mellor, 1987); details of this forecast system can be found in several reports and studies (Tallapragada et al., 2014; Yablonsky et al., 2015; Bender et al., 2019). The HWRF forecasts were previously used in studies of Hurricane Matthew (2016), looking at the hurricane's impact on disruption of the GS flow (Ezer et al., 2017), analyzing air-sea exchange under the hurricane (Ezer, 2018a) and evaluating the impact of hurricane track (Ezer, 2019a). The model results indicate that any hurricane track within a few hundred km from the path of the GS can cause a weakening in the GS flow with somewhat larger impact if the hurricane is located enough time just east of the GS so that the counter clockwise winds are blowing against the flow of the GS. The motivation for this study comes from the fact that the track of hurricane Dorian perfectly matched the optimal conditions for maximum impact on the GS and was similar to the track of the previously studied hurricane Matthew, giving us an opportunity to test whether or not the unusual impact of hurricane Matthew can be repeated by other hurricanes.

## 3. Results

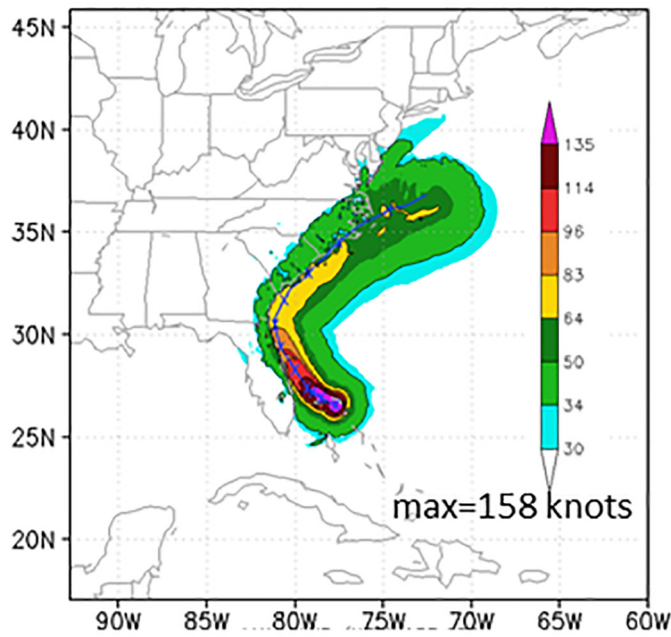
### 3.1. Surface currents, surface temperatures and sea surface height during Dorian

Fig. 2 shows the HWRF forecast of maximum winds and surface currents, September 2–6, 2019, when the hurricane moved along the coast of the South-Atlantic Bight (SAB) from Florida to South Carolina. When the eye of the storm was over the Bahamas in September 2 (Fig. 2b) the FC was relatively strong since the wind north of the Bahamas pushed waters northwestward toward the FC. However, when the hurricane moved closer to shore it clearly disrupted the flow, disconnecting the upstream FC from the downstream GS (Fig. 2b,c).

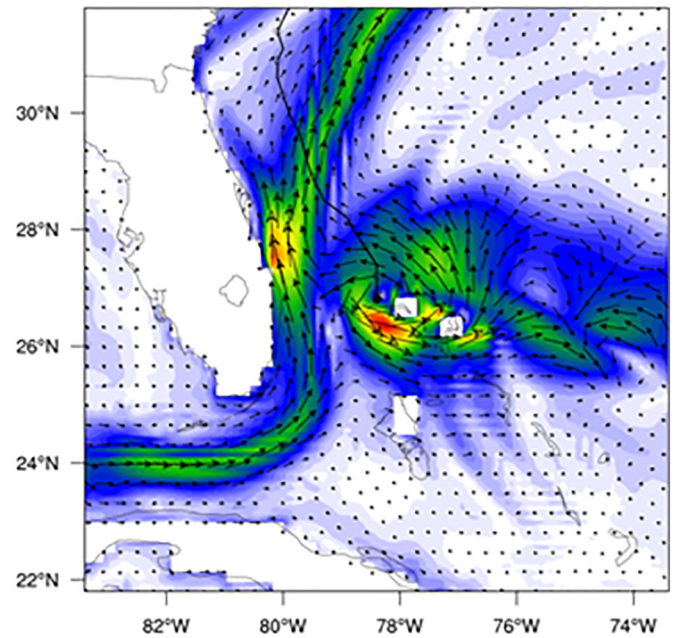
It is interesting to note that this disruption to the GS flow was very similar to the impact of hurricane Matthew when it was at almost the same location (for comparison, see Fig. 1 in Ezer et al., 2017). Beyond the direct impact of the hurricane on surface currents, Ezer et al. (2017)

### NOAA/HWRF forecast of hurricane Dorian

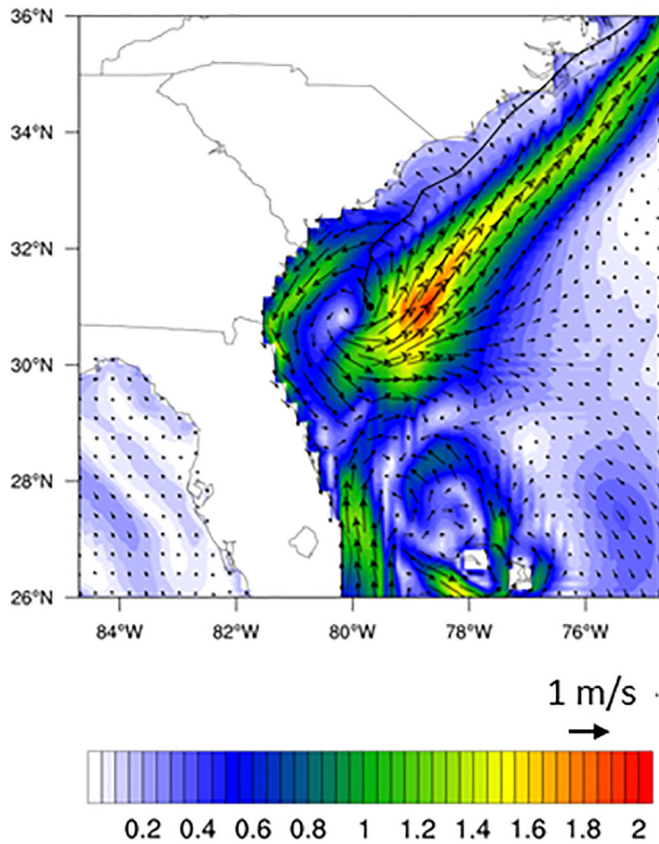
(a) Maximum wind September 2-6, 2019



(b) Surface currents September 3, 2019



(c) Surface currents September 5, 2019



(d) Surface currents September 6, 2019

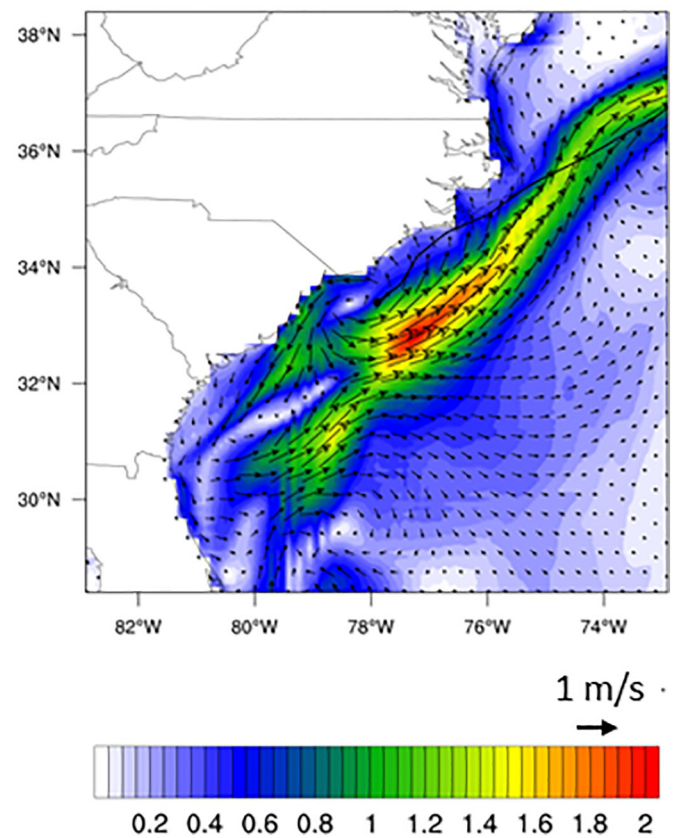
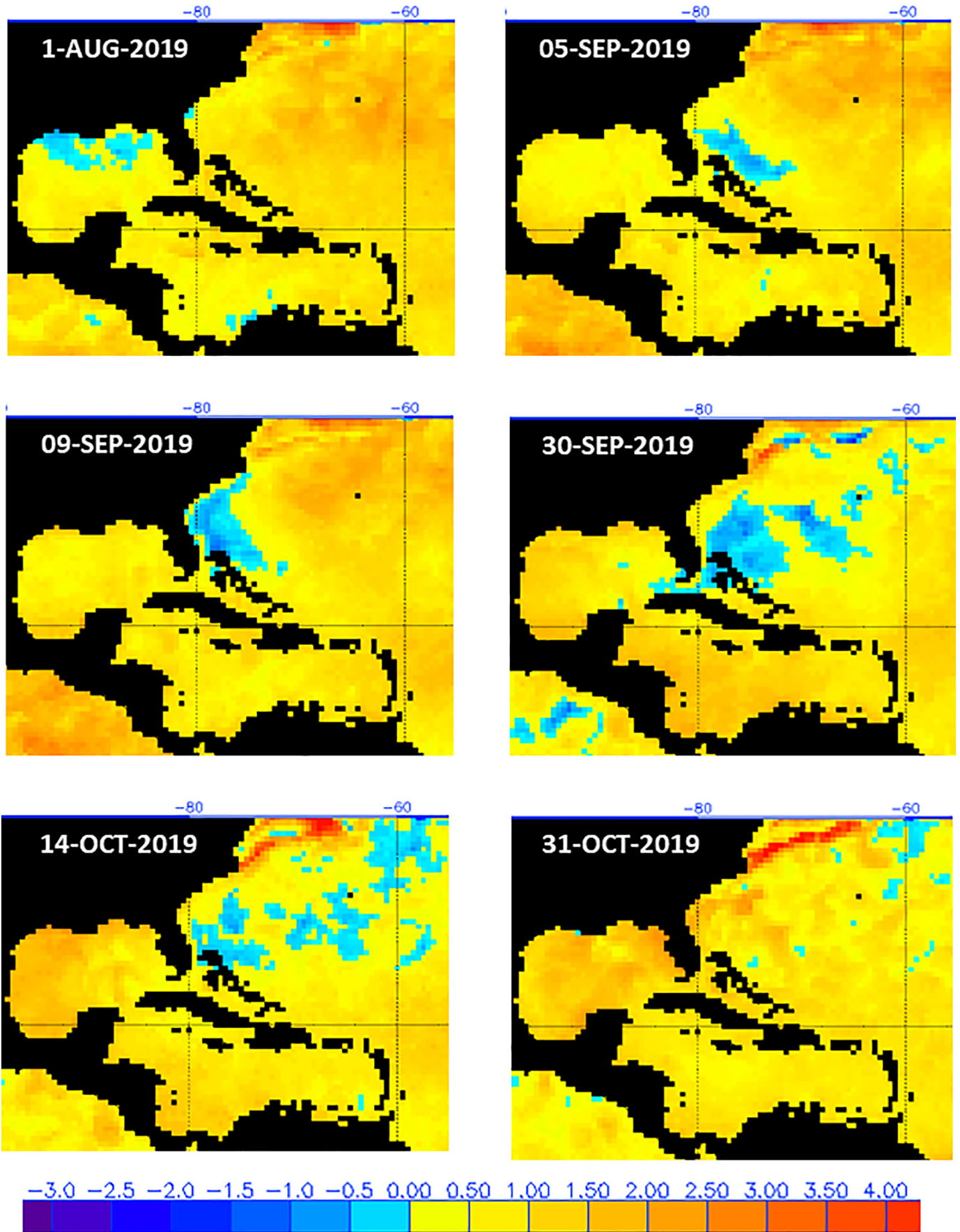


Fig. 2. Forecasts of hurricane Dorian from NOAA's operational ocean-hurricane coupled HWRF-POM model. (a) Maximum wind speed (knots) and track predicted for September 2-6, 2019. (b)-(d) Surface ocean currents for September 3, 5 and 6, respectively.

### NOAA/NESDIS SST Anomaly (°C)



(caption on next page)

**Fig. 3.** Sea Surface Temperature (SST) anomaly from NOAA/NESDIS analysis of satellite data for selected days, before hurricane Dorian (August 1st, 2019), during the hurricane (September 5–9th) and after the hurricane (September 30th to October 31st).

also showed how the hurricane's induced mixing eroded the stratification across the GS, which could have indirect consequences with long-lasting impacts.

The impact of the hurricane on SST can be seen in Fig. 3. About a month before Dorian became a hurricane (August 1st), the only negative SST anomaly was in the Gulf of Mexico (remnants of tropical storm Barry), but all the Atlantic and Caribbean areas had positive SST anomalies. During September 5–9, when the hurricane moved along the US coast, the track was followed by colder waters along the coast of the South Atlantic Bight (SAB). Ezer (2018a) showed that the cooling of ocean waters under hurricane Matthew involved two mechanisms, surface heat loss due to the strong winds, as well as vertical mixing and upwelling of deep colder waters. After the hurricane moved away in early September, colder than normal SST can be seen, both, offshore in the SAB and downstream the GS in the Mid-Atlantic Bight (MAB). The colder anomaly seen at  $\sim 50^\circ\text{W}$  on October 31st could be an anomaly that had been advected by the GS flow—this hypothesis will be tested later. In the weeks after the hurricane disappeared, the GS brought new warmer waters from low latitudes that reestablished the temperature gradients across the GS and the baroclinic structure of the flow; this advective process is relatively slow, so the GS flow can remain weaker than normal for a long time after the hurricane, as shown for hurricane Matthew (Ezer, 2018a, 2019a). It will be shown later that similar mechanism applied to Dorian as well.

Altimeter data is next used to evaluate the impact of the hurricane on the large-scale circulation. SSH over the North Atlantic Ocean over the 3 months of the study (Fig. 4, left panels) show the meandering GS as the region with the largest SSH gradients, since the GS separates between the high SSH (and warmer temperatures) over the subtropical gyre and the low SSH (and colder temperatures) over the subpolar gyre and along the U.S. coast. The geostrophic velocity derived from the SSH gradients clearly show the path of the GS as the dominant feature of the region (Fig. 4, right panels). Due to the GS meanders and mesoscale eddies there are considerable changes in the path and strength of the GS and further analysis will quantify these changes.

The GS can change due to meandering and changes in recirculation gyres on both sides of the stream, so large spatial variations can be found even between close sections across the stream, as shown for example from recent direct observations (Andres et al., 2019). It does seem that before the hurricane (Fig. 4, upper-right panel) strong flow (red) continues along the entire length of the GS, while in the following months there are sections with weaker flows. However, it is not yet clear if these changes are related or not to the impact of the hurricane, so further analysis later will look at possible signals that propagate along the track of the GS.

### 3.2. The impact of Dorian on coastal sea level

Several recent studies show higher than normal coastal sea level and increased flooding when the GS slows down, either due to natural oscillations or following an offshore storm that disrupts the GS flow (Ezer and Atkinson, 2014, 2017; Ezer, 2016, 2018a, 2018b, 2019a). Fig. 5 for example, shows the hourly sea level near Norfolk and the daily transport of the FC during the 3 months period of this study; other places along the coast show similar patterns. Note that during the entire 3-month period observed water level was above the predicted high tide (in average, 0.26 m above the Mean Higher High Water, MHHW), causing dozens of days with tidal flooding. The most severe flood ( $> 1$  m above MHHW) was during hurricane Dorian, but two other smaller storms near the GS, Humberto and Melissa (Fig. 1) also caused minor flooding (Fig. 5; top). Moreover, during the 3-month period, the FC had 3 minima in transport (Fig. 5; bottom) that coincided with these

3 storms. None of these storms came close to Norfolk, so these floods (so called “sunny day” or “nuisance “floods) are consistent with the past experience of coastal sea level rise when the GS is weakening.

The correlation between FC transport and coastal sea level is  $-0.5$  (like previous findings mentioned above), which means that about 25% of the coastal variability may be attributed to relation with the GS. As mentioned before, the largest drop in FC transport (to a record low of 17.1 Sv) was during hurricane Dorian in early September. Note that Norfolk experienced elevated water level and flooding in late August, more than a week before Dorian reached the Mid-Atlantic region—during this time Dorian was moving slowly over the Bahamas and the FC started dropping from its peak of  $\sim 35$  Sv to  $\sim 27$  Sv. Note also that September–October are the months of the year with the most flooding on the southeastern coasts of the U.S. due to the annual and semiannual tides that exacerbate the impact of storms (Ezer, 2019b).

Altimeter data is now analyzed to show how sea level changed along the entire coast during Dorian, using the grid cells closest to the coast (Fig. 6). During August, before Dorian moved toward the U.S. coast, sea level in the SAB was lower than normal, which is consistent with strong FC flow (Fig. 2b and Fig. 5). In the SAB, during the storm in early September storm surge elevated the water along the coast and water remained elevated for at least a month until middle October. In the MAB, and to some degree farther north in the Gulf of Maine (GOM), elevated water was seen for  $> 2$  months, at least until early November. Impact from the smaller storms Humberto and Melissa may have also contributed to the elevated sea level in late September and October. This lasting impact of hurricanes on elevated sea level has been seen before, for example, during hurricane Matthew (Ezer, 2018a, 2019a). The altimeter data along the coast (Fig. 6) are consistent with the tide gauge data (Fig. 5) though they underestimate the highest water peaks. Because of the change in topography and coastline there is a clear distinction in the response of sea level between the three regions (SAB, MAB and GOM); these spatial regional differences have been discussed in several studies (Ezer, 2013; Piecuch et al., 2016; Woodworth et al., 2016; Valle-Levinson et al., 2017; Domingues et al., 2018; Ezer, 2019c).

Anti-correlation between the FC transport and sea level in Norfolk is shown in Fig. 5 and several previous studies (Ezer, 2013, 2018b; Ezer and Atkinson, 2014, 2017); these studies used hourly tide gauge data, so it is constructive to know if daily  $\frac{1}{4}$  degree altimeter data can also detect similar relation between the FC and coastal sea level. Therefore, correlations are calculated between the daily FC transport at  $27^\circ\text{N}$  and SSH anomaly over the entire study area (Fig. 7). While the correlations are quite noisy offshore where mesoscale variability dominates, a pattern emerges along almost the entire coast, from Florida to Cape Code, where consistent negative correlations are found (dark blue in Fig. 7) that are statistically significant (correlations over 0.34 have at least 99% confidence level or  $p$ -value  $< .01$ ). Offshore, along the path of the GS there is positive correlation (red), which means that when the FC is weakening sea level is rising along the coast and falling offshore—i.e., the gradients of sea level across the GS are smaller (and geostrophic speed is smaller). The most significant correlations (darkest blue in Fig. 7) are found along the SAB coast and near the Chesapeake Bay (near Norfolk, Fig. 5), where the  $p$ -value is practically zero ( $P < 10^{-10}$ ). The correlations explain the results in Fig. 5 and Fig. 6 that show especially large increase in sea level around  $37^\circ\text{N}$ – $39^\circ\text{N}$  (the MAB, including Norfolk). The fact that there is only a very short lag between changes in the FC transport and coastal sea level response thousands of km away has been discussed before and demonstrated by a numerical model (Ezer, 2016). The changes in the GS flow create a fast moving large-scale barotropic sea level signal, and this signal when reaching the coast triggers coastal-trapped waves (Huthnance, 1978) that spread the signal along the coast and resulted in coherent sea level anomalies

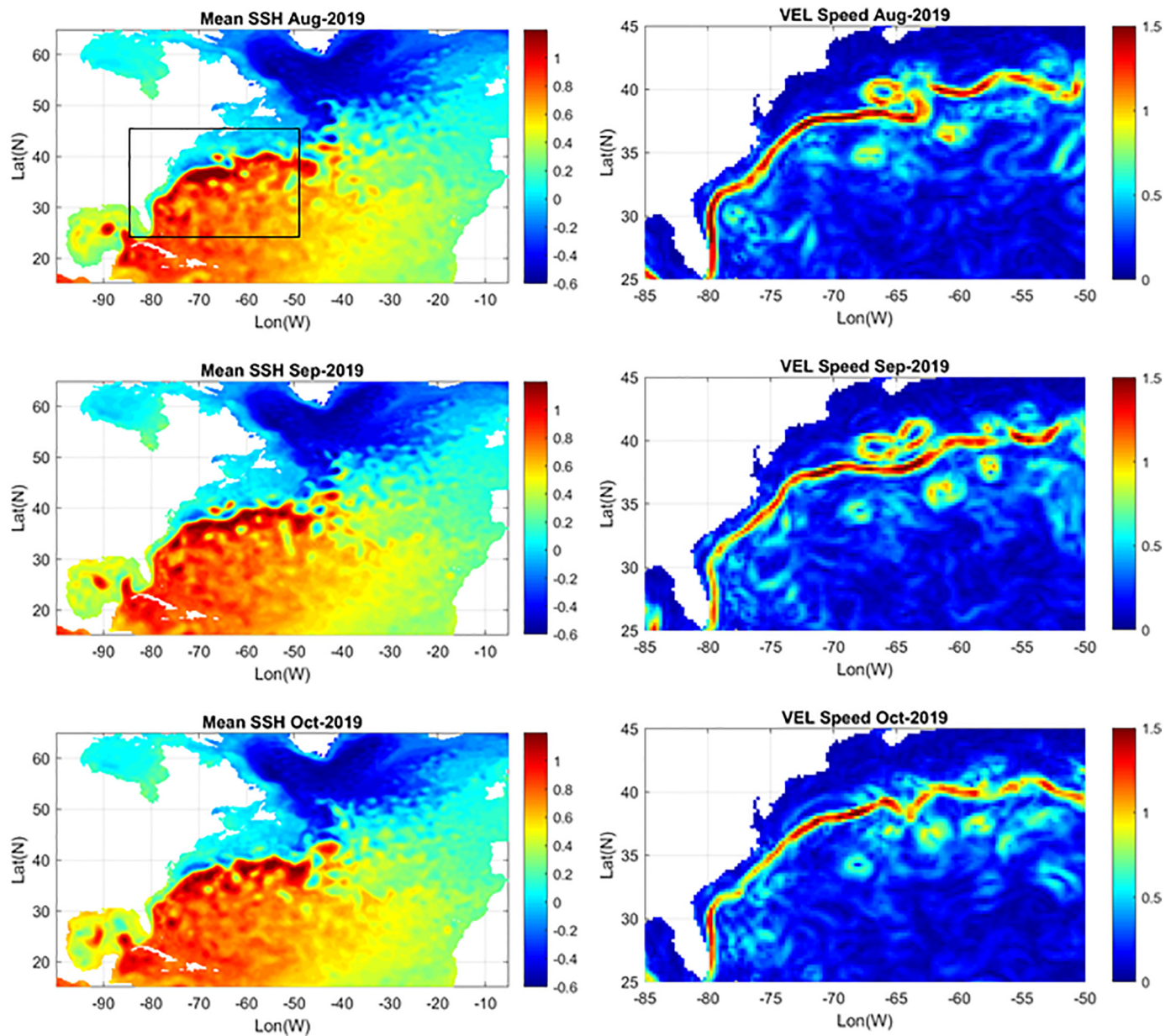


Fig. 4. Monthly means surface data from AVISO satellite altimeters for August–October 2019. Left panels- Sea Surface Height (SSH in m) in the North Atlantic Ocean. Right panels- surface geostrophic velocity speed (in m/s) in the Gulf Stream subregion shown in the box on the upper-left panel.

along large stretches of the coast, as seen here and in other coasts (Hughes and Meredith, 2006).

### 3.3. The impact of Dorian on the Gulf stream velocity

The daily paths of the GS during the three-month period were obtained from the maximum surface geostrophic velocity and shown in Fig. 8. There are only very small variations south of about 37°N, when the GS is close to the SAB coast and immediately after it separates from the coast at Cape Hatteras. Large variations in the position of the GS in the MAB region west of 70°W are associated with local recirculating gyres, meandering and eddies (Andres et al., 2019). The statistics of the velocity along the GS path (mean and standard deviation) are shown in Fig. 9a. The region with the strongest velocity and largest variability is around 62°W–72°W (some 1500–2500 km downstream), where GS meandering and eddy shedding dominate the flow (Fig. 4). The results here are consistent with direct observations of the GS which show for example larger variations in GS position and flow at 68.5°W than at

70.3°W (see Fig. 3 in Andres et al., 2019).

The impact of hurricane Dorian on the velocity of the GS is clearly seen in Fig. 9b where velocities along the GS track were averaged for two regions, the SAB and the MAB. As shown before (Figs. 2 and 5) the GS flow in the SAB increased just before the storm (mean over entire region  $\sim 1.55$  m/s) but then dropped sharply during the storm in early September (to  $\sim 1.05$  m/s); the flow in the SAB remained low for at least two months (until early November), with a very slow recovery. In the MAB on the other hand, the impact of Dorian is seen only later, about 2 weeks after the hurricane disappeared- from middle September to November the mean flow continued to drop. Therefore, an interesting result is that after the storm, flow intensified in the SAB but continued to weaken in the MAB. Ezer (2019c) found similar opposite trends between the SAB and MAB in both coastal sea level and GS velocity, which was explained by time lag of propagation of thermal anomalies that are advected along the path of the GS. Fig. 9b may also show some small contribution in reducing the flow following hurricane Humberto in late September and tropical storm Melissa in October (like

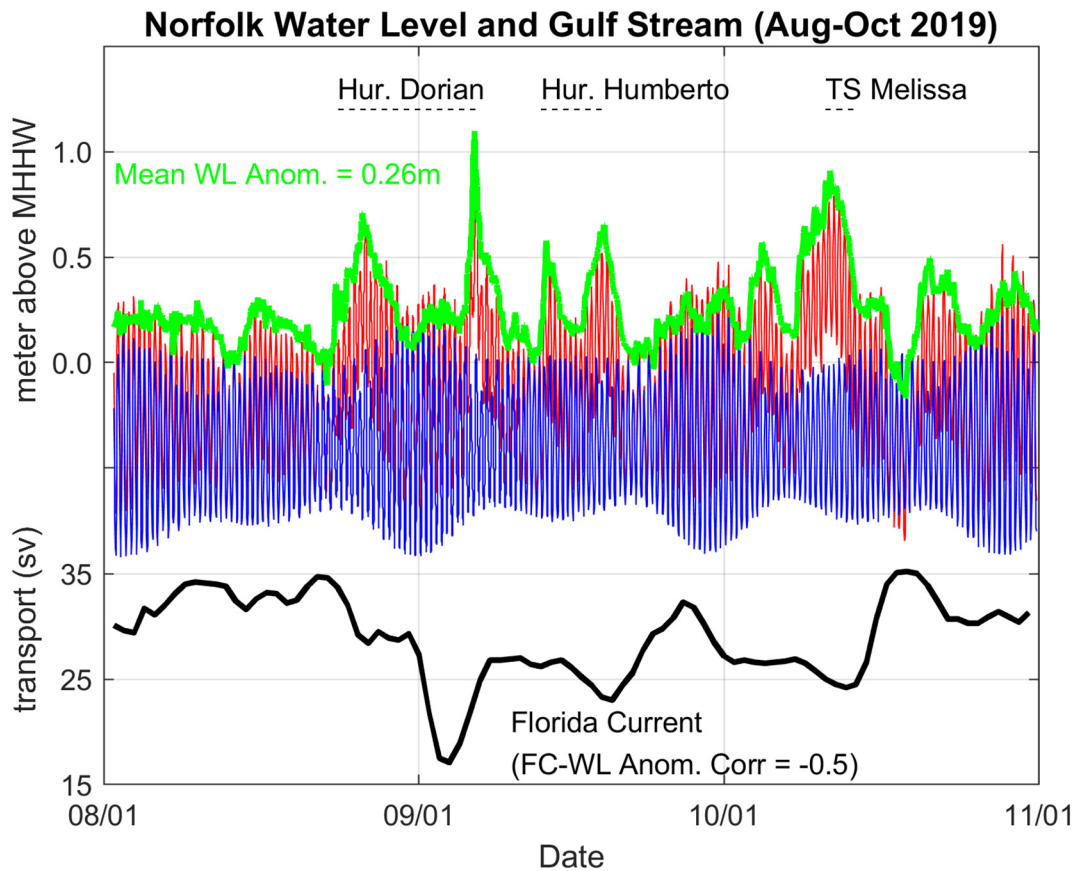


**Fig. 5.** Top- hourly sea level from the tide gauge in Norfolk (76.33°W, 36.95°N). In blue, red and green are tide prediction, observed sea level and residual anomaly (observed minus tide), respectively. Time of hurricane Dorian and two other smaller storms in the region are shown. Bottom- observed Florida Current transport at 27°N ( $1 \text{ Sv} = 10^6 \text{ m}^3/\text{s}$ ). (For interpretation of the references to colour in this figure legend, the reader is referred to the web version of this article.)

the impact on the FC seen in Fig. 5).

In Fig. 10 the correlation between the FC transport and the GS flow downstream is shown (with different lags from 0 to 50 days). Most of the significant correlations (red stars signify  $p$ -value  $< .05$ ) between the FC and the downstream GS with zero lag (top panel of Fig. 10) are found within  $\sim 600$  km of the FC measurements, but correlations with increasing lag indicate clear downstream propagation of signals. For example, the highest correlations are found  $\sim 500$ – $1300$  km downstream after 20 days,  $2000$ – $2500$  km downstream after 30 days and  $3000$ – $3700$  km downstream after 50 days. This propagation speed of about  $1 \text{ m/s}$  is consistent with the speed of advection by the GS. There is also significant correlation and slower propagation of signals within the SAB, so that the northern portion of the SAB (just south of Cape Hatteras) is correlated with the FC transport 50 days earlier; this signal is propagating much slower, at  $\sim 0.1 \text{ m/s}$  and will be discussed later.

Another way to show propagating signals is using the Hovmöller diagram in Fig. 11, where the velocity anomaly along the GS paths is shown as a function of time and distance - the two main propagation signals discussed above are highlighted by the dash lines, but other propagating signals can also be seen. The impact of hurricane Dorian on reducing velocity (blue in Fig. 11) at the beginning of September seemed to trigger the two main propagating signals. The faster propagating signal in the MAB reached  $\sim 4000$  km downstream within  $\sim 50$  days ( $\sim 0.9 \text{ m/s}$ ) and is consistent with advection by the GS of the cold anomaly created by the hurricane (see SST on 31-October in Fig. 3). The slower propagating signal within the SAB moved only  $\sim 500$  km during  $\sim 50$  days after the storm (speed of  $\sim 0.1$ – $0.15 \text{ m/s}$ ); there are also other slow-moving signals with similar propagation speeds and long wavelengths that are not as pronounced. The typical size of tropical cyclones and the length scale of their pressure field

(Chavas et al., 2016) are of the same order as the wavelength of propagating signals seen in Fig. 11, but further research on the relation between storm-induced atmospheric disturbances and large-scale ocean waves is needed. The mechanism involved in the changes within the SAB and the slow-moving signals are not so clear, but probably involve baroclinic processes. Ezer et al. (2017) showed that in the SAB near the storm, deep mixing and upwelling impacted the entire water column, so that for deep layers where velocities are much weaker than the surface layers of the GS, advective processes are slower and the density anomaly may induce baroclinic waves. Hansen (1970) and Johns (1988) for example, suggested a possible mechanism for slow-moving propagation signals of meanders along the GS which involve baroclinic instability theory and quasi-geostrophic waves with wavelength of  $200$ – $400$  km and propagation speed of  $\sim 0.1$ – $0.2 \text{ m/s}$  (i.e., with similar characteristics to the waves seen in Fig. 11), but faster moving waves ( $\sim 0.3$ – $0.5 \text{ m/s}$ ) were also observed. Theoretical and numerical modeling of baroclinic instability by Xue and Mellor (1993), show that the most unstable waves in the SAB have wavelength of  $\sim 200$  km and propagation speed of  $\sim 0.4 \text{ m/s}$ ; the instability is affected by the topography, which may explain some of the differences between the SAB and MAB. It is thus quite possible that the disruption to the GS structure caused by the storms triggered barotropic and baroclinic instability waves as observed here and in previous studies. Having observations of the entire water column during and after the storm (not an easy task) would be useful to better understand these processes in future studies and using numerical models would certainly help to study the generation and propagation of waves along the GS path.

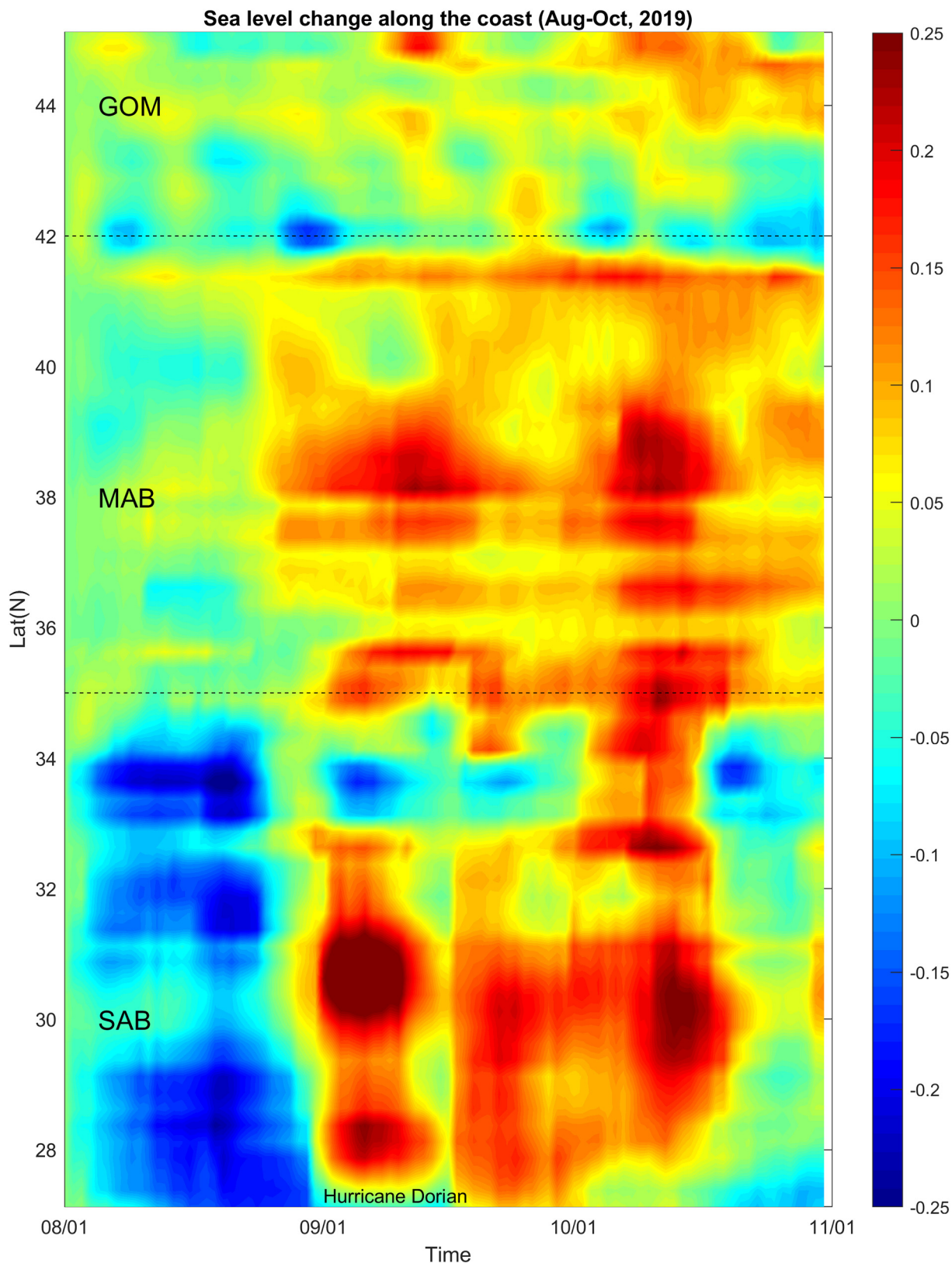


Fig. 6. Sea level change (in m) along the coast as a function of time and latitude. The sea level change is from the altimeter data points closest to the coast and shows change relative to the sea level on August 1, 2019. Three regions are separated by the dash lines, South-Atlantic Bight (SAB), Mid-Atlantic Bight (MAB) and Gulf of Maine (GOM); also shown is the time when hurricane Dorian was close to the coast.

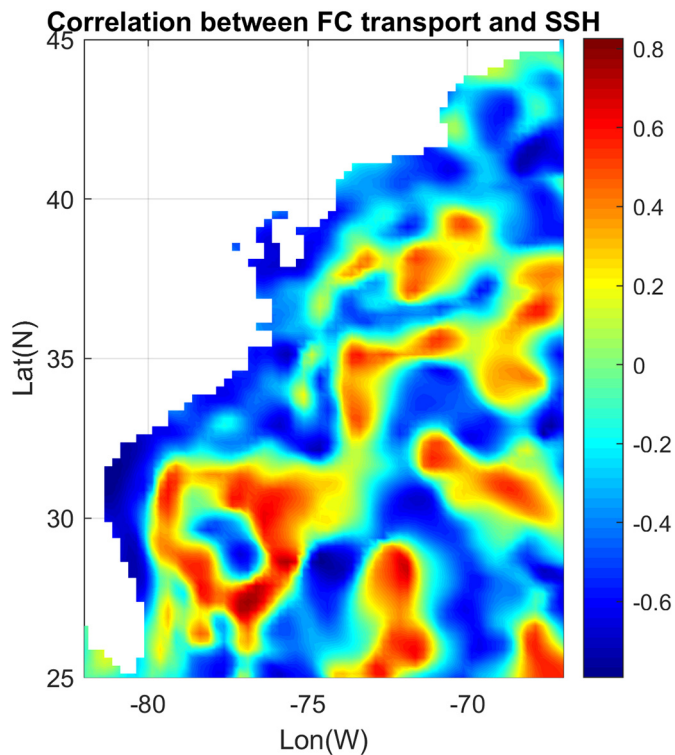


Fig. 7. Correlation coefficient between the daily Florida Current (FC) transport at 27°N and SSH from the altimeter data. Absolute value of correlations above 0.34 have  $p$ -value  $< .01$  (confidence level  $> 99\%$ ).

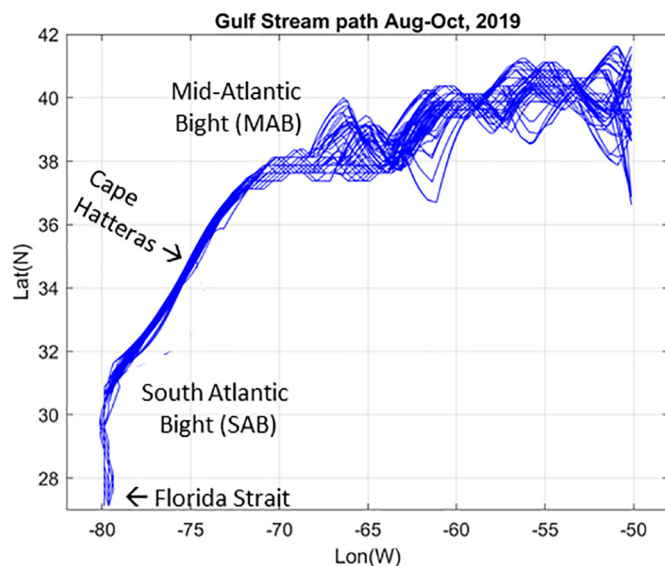


Fig. 8. Daily Gulf Stream paths for August–October 2019, obtained from the maximum surface geostrophic velocity in the altimeter data.

#### 4. Summary and conclusions

Sea level rise and associated acceleration in the frequency and severity of flooding (Ezer and Atkinson, 2014; Park and Sweet, 2015) is an issue of great concern for coastal communities along the U.S. East Coast from Boston (Kruegel, 2016) to Miami (Wdowinski et al., 2016). Linear sea level rise rates are much higher in this region than global rates, especially in the Mid-Atlantic area (Ezer, 2013) due to land subsidence (Karegar et al., 2017; Fiaschi and Wdowinski, 2019), so both, minor floods (so called “Nuisance floods” or “sunny day floods”)

as well as storm surge floods have dramatically increased in recent decades. Minor storms that had little impact in the past, now with the additional sea level rise, can cause significant flooding. Non-linear variations in sea level, such as decadal variations and sudden regional acceleration that creates “hotspots” (Goddard et al., 2015; Valle-Levinson et al., 2017; Domingues et al., 2018; Ezer, 2019c) make prediction of future sea level rise more difficult. Important contributors to coastal sea level variability such as offshore remote influence from atmospheric (e.g., pressure and wind) and oceanic (e.g., meridional overturning circulation, local currents and basin-scale waves) forcing are not fully understood to include them in coastal sea level predictions. In particular, in recent years there is growing evidence that when the GS weakens, coastal sea level rises and more floods are observed; this phenomenon occurs on a wide range of scales from daily natural oscillations (Ezer, 2016) to decadal variations (Ezer et al., 2013) and recently found GS variations induced by storms (Ezer, 2019a). The goal of this study was to better understand the mechanism and extent of the latter phenomena using observations taken before, during and after the passage of one of the strongest Atlantic storms, hurricane Dorian (August 28 to September 6, 2019).

A dramatic example of the impact of storms on the GS was hurricane Matthew (2016) which resulted in weakening of the GS flow by almost 50%, as seen from the cable measurements of the FC, from high-frequency radar of surface currents off Cape Hatteras and from a coupled hurricane-ocean model (Ezer et al., 2017); this led to further research on hurricane Matthew using ocean models (Ezer, 2018a, 2019a). These studies, as well as further observations by gliders of the impact of hurricanes on the GS in 2017 (Todd et al., 2018) all showed that storms may have a long-lasting impact, whereas a weaker than normal GS that can last for weeks after storms can increase flooding after storms disappear. Since hurricanes are rare occurrences it is almost impossible to repeat experiments, but then in the fall of 2019, hurricane Dorian followed the unusual track of hurricane Matthew along the GS and the coast of the SAB, with even greater impact on the GS. The FC transport was not only reduced by almost 50% (like during Matthew) but also weakened to its lowest recorded level (17.1 Sv) since observations began in 1982 (Baringer and Larsen, 2001). The NOAA’s coupled hurricane-ocean forecast model and altimeter data analyzed here showed how Dorian disrupted the GS flow- the FC first increased its flow when the hurricane was approaching the Bahamas and pushed water toward the Florida Straits, but then when the hurricane was near the GS, the winds were blowing against the currents, thus slowing down the GS flow. This direct effect on surface currents was also followed by intense surface cooling (seen by SST data) and mixing of the upper layers (like during Matthew; Ezer et al., 2017). Hurricanes, with their low surface air pressure (Fig. 1) can also have significant effect on sea level (Piecuch et al., 2016), though since the air pressure gradient is proportional to the wind speed, it is difficult to separate between the wind and pressure impacts. Due to the inverted barometer (IB) effect, surface pressure near the eye of the storm (Fig. 1b) can be some 50mb lower than outside the storm, temporally raising sea level there by  $\sim 50$  cm. Though it is difficult to evaluate how the IB may affect the GS dynamics, this impact is a barotropic process that is not likely to last longer than hours, compared with the long-lasting baroclinic impact due to the hurricane-induced mixing and cooling, as describe before.

To study the extent of the impact, analysis of altimeter data was conducted both, along the coast and along the path of the GS. Along the coast, the impact on raising sea level was seen immediately after Dorian approached the Florida coast- this impact is due to the fast barotropic response of sea level (Ezer, 2016). Coastal sea level remained anomalously high for over two months, as seen by tide gauge data (Fig. 5) and altimeter data (Fig. 6). On the other hand, the response along the path of the GS is a slower baroclinic process where cold anomalies created by the hurricane in the SAB propagated downstream at  $\sim 1$  m/s, reaching distance of  $\sim 4000$  km from the Florida Strait within  $\sim 50$  days. The dynamic process is as follows. When the hurricane mixes

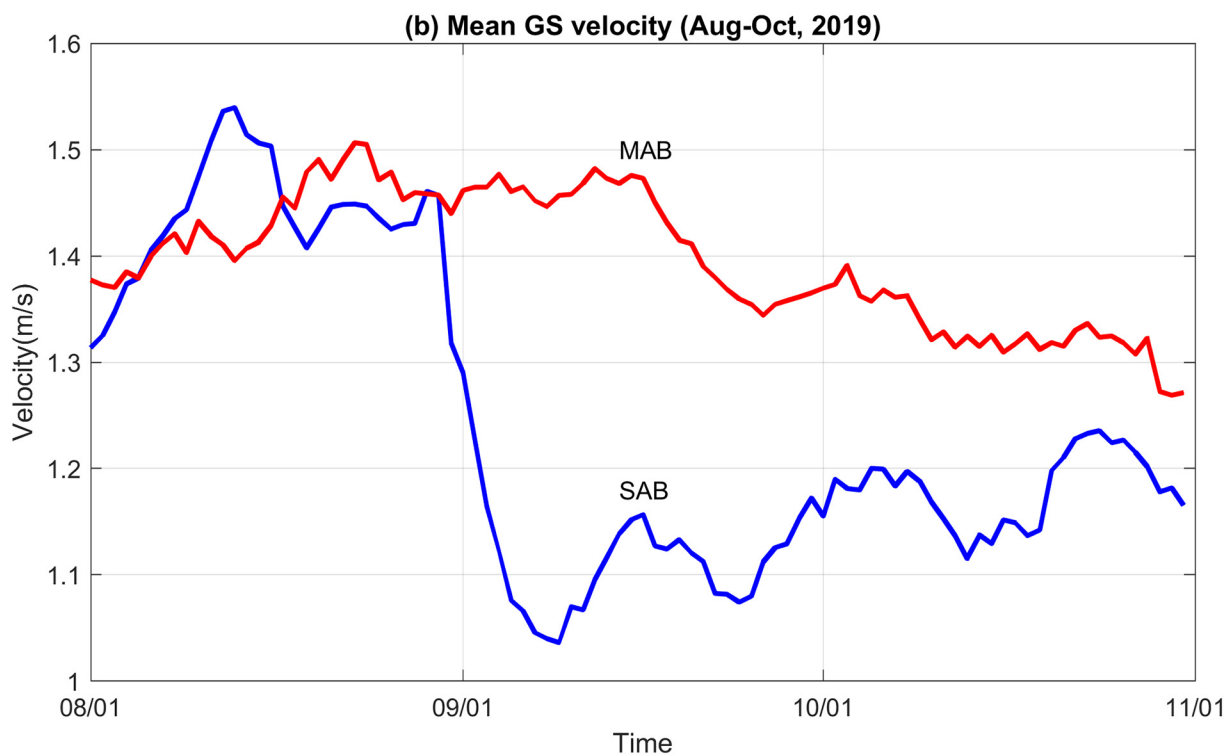
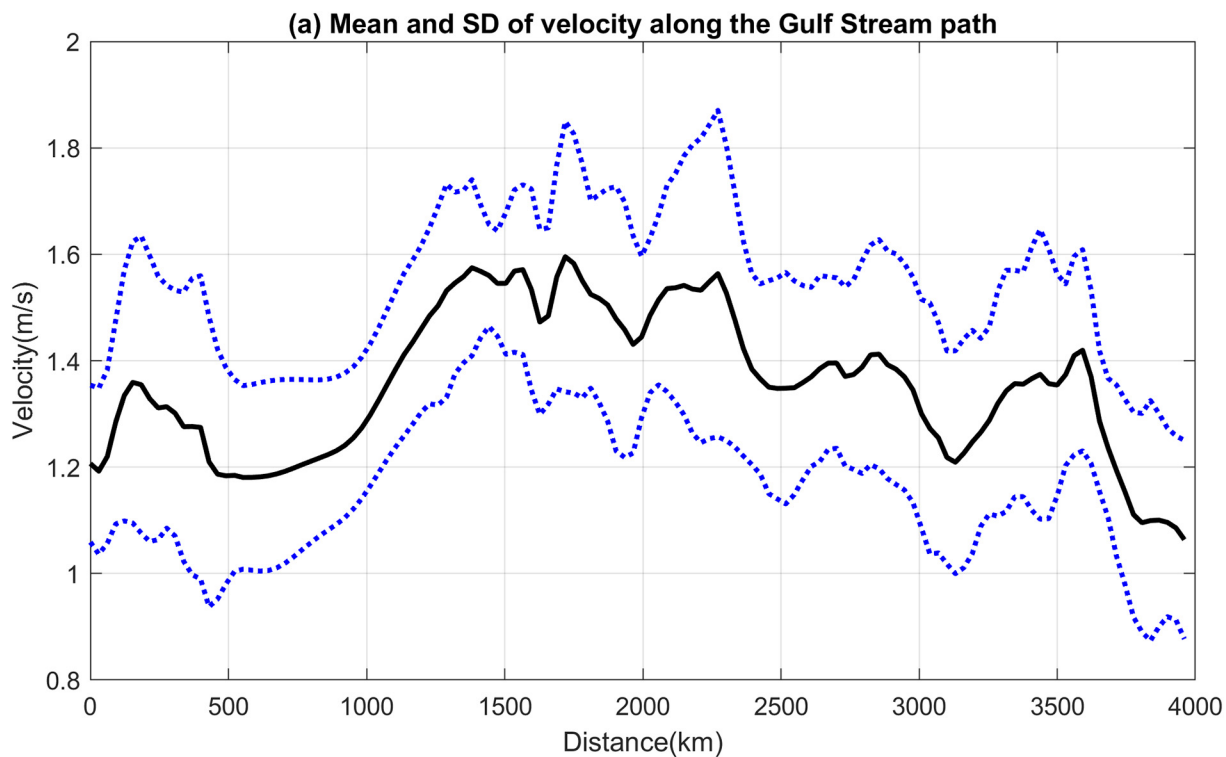


**Fig. 9.** (a) Mean (black line) and standard deviation (dash blue lines) of velocity along the GS path, calculated from the daily velocities. (b) Mean GS velocity as a function of time for the SAB (blue line) and the MAB (red line) regions (south and north of 35°N, respectively). (For interpretation of the references to colour in this figure legend, the reader is referred to the web version of this article.)

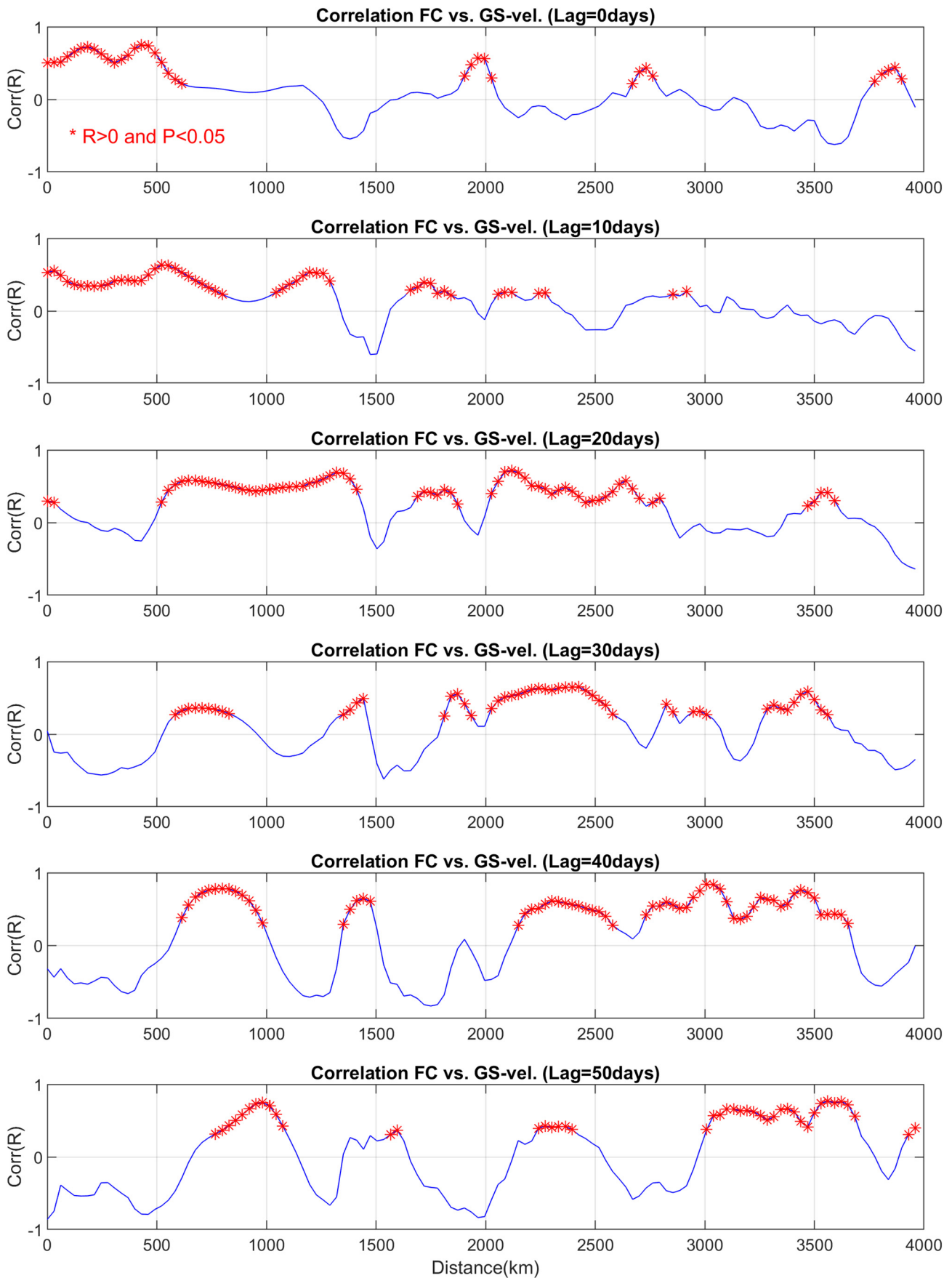


**Fig. 10.** Correlation between the FC transport (Fig. 5) and the velocity along the GS paths (Fig. 9). Positive correlations with statistical significance over 95% are marked by red stars. From the top to bottom are calculations with different lags from zero to 50 days. (For interpretation of the references to colour in this figure legend, the reader is referred to the web version of this article.)

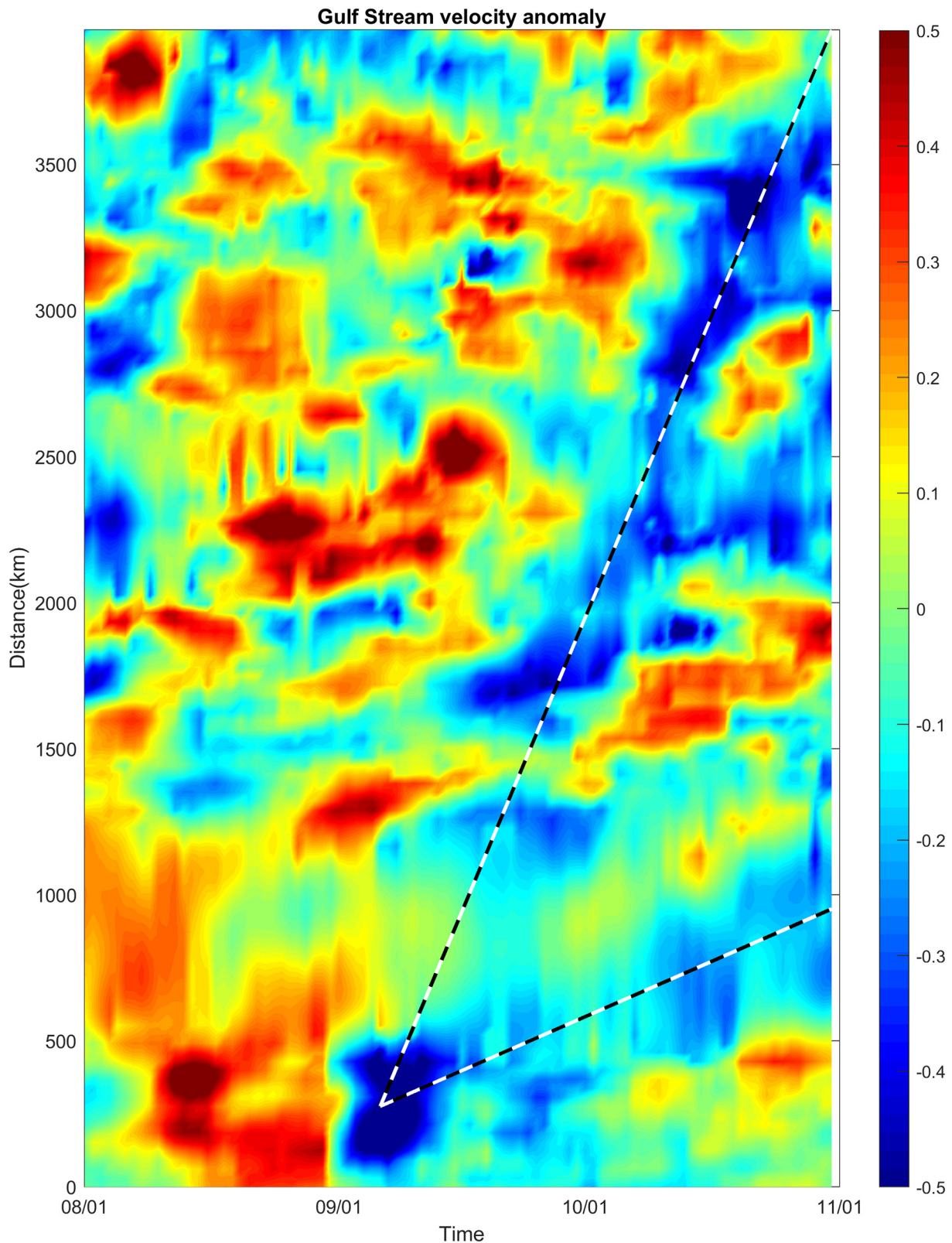


Fig. 11. Gulf Stream velocity anomaly (in m/s) as a function of time and distance along the GS path. Two dash lines represent potential propagation of negative anomalies from the hurricane time in early September to the SAB (the shorter line that stretches to ~1000 km) and MAB (the longer line that stretches to ~4000 km).

the upper layers and cools the warm GS waters, the thermal (and density) gradients across the stream are degraded, thus reducing the baroclinic geostrophic velocity portion of the GS. Then this anomaly of cold water (and lower velocity) is propagating downstream along the path of the GS and later replaced by warmer waters brought from the

south, until the stratification and the sharp front is rebuilt. This process can take up to 2 months, as seen in the observations here and demonstrated by numerical models (Ezer, 2018a, 2019a). In addition to the advective propagation (at ~1 m/s), the hurricane may also trigger baroclinic instability waves near the GS (Xue and Mellor, 1993) and

slow-moving ( $\sim 0.1$  m/s) baroclinic waves similar to waves and meanders previously observed moving along the GS path (Hansen, 1977; Johns, 1988).

The results of this study about lasting impact of storms and the extent of their indirect impact may have important implications for the variability of large-scale ocean circulation, coastal sea level rise and possibly ecosystems such as marshlands (Neubauer et al., 2019; Tully et al., 2019). Further studies using models and direct observations before and after storms could shed more light on these processes.

## Acknowledgments

The study is part of Old Dominion University's Climate Change and Sea Level Rise Initiative at the Institute for Coastal Adaptation and Resilience (ICAR). The Center for Coastal Physical Oceanography (CCPO) provided computational support. Bob Tuleya is thanked for discussions about hurricane models and two reviewers are thanked for many useful suggestions. Sources of publicly available data are: SST data (<https://www.nesdis.noaa.gov/>), satellite altimeter data (<http://las.aviso.oceanobs.com/las/>), hourly tide gauge sea level data (<http://opendap.co-ops.nos.noaa.gov/dods/>), Florida Transport data (<http://www.aoml.noaa.gov/phod/floridacurrent/>) and HWRF model forecasts data ([http://www.emc.ncep.noaa.gov/gc\\_wmb/vxt/HWRF/](http://www.emc.ncep.noaa.gov/gc_wmb/vxt/HWRF/)).

## References

- Andres, M., Donohue, K.A., Toole, J.M., 2019. The Gulf Stream's path and time-averaged velocity structure and transport at 68.5°W and 70.3°W. *Deep-Sea Res Part-1*. <https://doi.org/10.1016/j.dsr.2019.103179>.
- Baringer, M.O., Larsen, J.C., 2001. Sixteen years of Florida current transport at 27°N. *Geophys. Res. Lett.* 28 (16), 3179–3182. <https://doi.org/10.1029/2001GL013246>.
- Bender, M.A., Ginis, I., 2000. Real-case simulations of hurricane-ocean interaction using a high-resolution coupled model: effects on hurricane intensity. *Mon. Wea. Rev.* 128, 917–946. [https://doi.org/10.1175/1520-0493\(2000\)128<0917:RCOHO>2.0.CO;2](https://doi.org/10.1175/1520-0493(2000)128<0917:RCOHO>2.0.CO;2).
- Bender, M.A., Marchok, T., Tuleya, R.E., Ginis, I., Tallapragada, V., Lord, S.J., 2019. Hurricane model development at GFDL: a collaborative success story from a historical perspective. *Bull. Amer. Met. Soc.* 1725–1736. <https://doi.org/10.1175/BAMS-D-18-0197.1>. September 2019.
- Blumberg, A.F., Mellor, G.L., 1987. A description of a three-dimensional coastal ocean circulation model. In: Heaps, N.S. (Ed.), *Three Dimensional Coastal Ocean Models Vol 4*, Coastal and Estuarine Sci. AGU Publication. <https://doi.org/10.1029/CO004p000>.
- Boon, J.D., 2012. Evidence of sea level acceleration at U.S. and Canadian tide stations, Atlantic coast, North America. *J. Coast. Res.* 28 (6), 1437–1445. <https://doi.org/10.2112/JCOASTRES-D-12-00102.1>.
- Chavas, D.R., Lin, N., Dong, W., Lin, Y., 2016. Observed tropical cyclone size revisited. *J. Clim.* 29, 2923–2939. <https://doi.org/10.1175/JCLI-D-15-0731.1>.
- Domingues, R., Goni, G., Baringer, M., Volkov, D., 2018. What caused the accelerated sea level changes along the U.S. East Coast during 2010–2015? *Geophys. Res. Lett.* <https://doi.org/10.1029/2018GL081183>.
- Ezer, T., 2013. Sea level rise, spatially uneven and temporally unsteady: why the U.S. East Coast, the global tide gauge record, and the global altimeter data show different trends. *Geophys. Res. Lett.* 40, 5439–5444. <https://doi.org/10.1002/2013GL057952>.
- Ezer, T., 2015. Detecting changes in the transport of the Gulf Stream and the Atlantic overturning circulation from coastal sea level data: the extreme decline in 2009–2010 and estimated variations for 1935–2012. *Glob Planet Change* 129, 23–36. <https://doi.org/10.1016/j.gloplacha.2015.03.002>.
- Ezer, T., 2016. Can the Gulf Stream induce coherent short-term fluctuations in sea level along the U.S. East Coast?: a modeling study. *Ocean Dyn.* 66 (2), 207–220. <https://doi.org/10.1007/s10236-016-09280>.
- Ezer, T., 2018a. On the interaction between a hurricane, the Gulf stream and coastal sea level. *Ocean Dyn.* 68, 1259–1272. <https://doi.org/10.1007/s10236-018-1193-1>.
- Ezer, T., 2018b. The increased risk of flooding in Hampton Roads: on the roles of sea level rise, storm surges, hurricanes and the Gulf Stream. *Mar Tech Soc J* 52 (2), 34–44. <https://doi.org/10.4031/MTSJ.52.2.6>.
- Ezer, T., 2019a. Numerical modeling of the impact of hurricanes on ocean dynamics: sensitivity of the Gulf Stream response to storm's track. *Ocean Dyn.* 69 (9), 1053–1066. <https://doi.org/10.1007/s10236-019-01289-9>.
- Ezer, T., 2019b. Analysis of the changing patterns of seasonal flooding along the U.S. East Coast. *Ocean Dyn.* <https://doi.org/10.1007/s10236-019-01326-7>.
- Ezer, T., 2019c. Regional differences in sea level rise between the Mid-Atlantic Bight and the South Atlantic Bight: is the Gulf Stream to blame? *Earth's Future* 7 (7), 771–783. <https://doi.org/10.1029/2019EF001174>.
- Ezer, T., Atkinson, L.P., 2014. Accelerated flooding along the U.S. East Coast: on the impact of sea-level rise, tides, storms, the Gulf Stream, and the North Atlantic Oscillations. *Earth's Future* 2 (8), 362–382. <https://doi.org/10.1002/2014EF000252>.
- Ezer, T., Atkinson, L.P., 2017. On the predictability of high water level along the U.S. East Coast: can the Florida Current measurement be an indicator for flooding caused by remote forcing? *Ocean Dyn.* 67 (6), 751–766. <https://doi.org/10.1007/s10236-017-1057-0>.
- Ezer, T., Corlett, W.B., 2012. Is sea level rise accelerating in the Chesapeake Bay? A demonstration of a novel new approach for analyzing sea level data. *Geophys. Res. Lett.* 39, L19605. <https://doi.org/10.1029/2012GL053435>.
- Ezer, T., Atkinson, L.P., Corlett, W.B., Blanco, J.L., 2013. Gulf Stream's induced sea level rise and variability along the U.S. mid-Atlantic coast. *J. Geophys Res Oceans* 118, 685–697. <https://doi.org/10.1002/jgrc.20091>.
- Ezer, T., Atkinson, L.P., Tuleya, R., 2017. Observations and operational model simulations reveal the impact of Hurricane Matthew (2016) on the Gulf Stream and coastal sea level. *Dyn Atmos Oceans* 80, 124–138. <https://doi.org/10.1016/j.dynatmoce.2017.10.006>.
- Fiaschi, S., Wdowinski, S., 2019. Local land subsidence in Miami Beach (FL) and Norfolk (VA) and its contribution to flooding hazard in coastal communities along the U.S. Atlantic coast. *Ocean Coast. Manag.* <https://doi.org/10.1016/j.ocecoaman.2019.105078>.
- Gawarkiewicz, G., Todd, R., Plueddemann, A., Andres, M., Manning, J.P., 2012. Direct interaction between the Gulf Stream and the shelfbreak south of New England. *Sci. Rep.* 2 (553). <https://doi.org/10.1038/srep00553>.
- Goddard, P.B., Yin, J., Griffies, S.M., Zhang, S., 2015. An extreme event of sea-level rise along the northeast coast of North America in 2009–2010. *Nature Comm* 6, 6345. <https://doi.org/10.1038/ncomms7346>.
- Hansen, D.V., 1970. Gulf stream meanders between Cape Hatteras and the Grand Banks. *Deep-Sea Res.* 17 (3), 495–511. [https://doi.org/10.1016/0011-7471\(70\)90064-1](https://doi.org/10.1016/0011-7471(70)90064-1).
- Hoarfrost, A., Balmonte, J.P., Ghobrial, S., Zierovell, K., Bane, J., Gawarkiewicz, G., Arnosti, C., 2019. Gulf Stream ring water intrusion on the Mid-Atlantic Bight continental shelf break affects microbially driven carbon cycling. *Front. Mar. Sci.* <https://doi.org/10.3389/fmars.2019.00394>.
- Hughes, C.W., Meredith, P.M., 2006. Coherent sea-level fluctuations along the global continental slope. *Philos. Trans. R. Soc.* 364, 885–901. <https://doi.org/10.1098/rsta.2006.1744>.
- Huthnance, J.M., 1978. On coastal trapped waves: analysis and numerical calculation by inverse iteration. *J. Phys. Oceanogr.* 8, 74–92. [https://doi.org/10.1175/1520-0485\(1978\)008<0074:OCTWAA>2.0.CO;2](https://doi.org/10.1175/1520-0485(1978)008<0074:OCTWAA>2.0.CO;2).
- Johns, W.E., 1988. One-dimensional baroclinically unstable waves on the Gulf Stream potential vorticity gradient near Cape Hatteras. *Dyn. Atmos. Oceans* 11 (3–4), 323–350. [https://doi.org/10.1016/0377-0265\(88\)90005-X](https://doi.org/10.1016/0377-0265(88)90005-X).
- Karegar, M.A., Dixon, T.H., Malservisi, R., Kusche, J., Engelhart, S.E., 2017. Nuisance flooding and relative sea-level rise: the importance of present-day land motion. *Sci. Rep.* 7, 11197. <https://doi.org/10.1038/s41598-017-11544-y>.
- Kourafalou, V.H., Androulidakis, Y.S., Halliwell, G.R., Kang, H.S., Mehari, M.M., Le Hénaff, M., Atlas, R., Lumpkin, R., 2016. North Atlantic Ocean OSSE system development: Nature Run evaluation and application to hurricane interaction with the Gulf Stream. *Prog. Oceanogr.* 148, 1–25. <https://doi.org/10.1016/j.pocean.2016.09.001>.
- Kruegel, S., 2016. The impacts of sea-level rise on tidal flooding in Boston, Massachusetts. *J. Coast. Res.* 32 (6), 1302–1309. <https://doi.org/10.2112/JCOASTRES-D-15-00100.1>.
- Li, Y., Xue, H., Bane, J.M., 2002. Air-sea interactions during the passage of a winter storm over the Gulf stream: a three-dimensional coupled atmosphere-ocean model study. *J. Geophys Res Oceans* 107 (C11). <https://doi.org/10.1029/2001JC001161>.
- Liu, X., Wei, J., 2015. Understanding surface and subsurface temperature changes induced by tropical cyclones in the Kuroshio. *Ocean Dyn.* 65 (7), 1017–1027. <https://doi.org/10.1007/s10236-015-0851-9>.
- Meinen, C.S., Baringer, M.O., Garcia, R.F., 2010. Florida Current transport variability: an analysis of annual and longer-period signals. *Deep Sea Res* 57 (7), 835–846. <https://doi.org/10.1016/j.dsr.2010.04.001>.
- Neubauer, S.C., Piehler, M.F., Smyth, A.R., Franklin, R.B., 2019. Saltwater intrusion modifies microbial community structure and decreases denitrification in tidal freshwater marshes. *Ecosystems* 22 (4), 912–928. <https://doi.org/10.1007/s10021-018-0312-7>.
- Oey, L.Y., Ezer, T., Wang, D.P., Fan, S.J., Yin, X.Q., 2006. Loop Current warming by Hurricane Wilma. *Geophys. Res. Lett.* 33, L08613. <https://doi.org/10.1029/2006GL025873>.
- Oey, L.Y., Ezer, T., Wang, D.P., Yin, X.Q., Fan, S.J., 2007. Hurricane-induced motions and interaction with ocean currents. *Cont. Shelf Res.* 27, 1249–1263. <https://doi.org/10.1016/j.csr.2007.01.008>.
- Park, J., Sweet, W., 2015. Accelerated sea level rise and Florida current transport. *Ocean Sci.* 11, 607–615. <https://doi.org/10.5194/os-11-607-2015>.
- Piecuch, C.G., Dangendorf, S., Ponte, R., Marcos, M., 2016. Annual sea level changes on the North American Northeast Coast: influence of local winds and barotropic motions. *J. Clim.* 29, 4801–4816. <https://doi.org/10.1175/JCLI-D-16-0048.1>.
- Sallenger, A.H., Doran, K.S., Howd, P., 2012. Hotspot of accelerated sea-level rise on the Atlantic coast of North America. *Nat. Clim. Change* 2, 884–888. <https://doi.org/10.1038/NCCLIMATE1597>.
- Shay, L.K., Goni, G.J., Black, P.G., 2000. Effects of a warm oceanic feature on hurricane Opal. *Mon Wea Rev* 128, 1366–1383. [https://doi.org/10.1175/1520-0493\(2000\)128<1366:EOAWOF>2.0.CO;2](https://doi.org/10.1175/1520-0493(2000)128<1366:EOAWOF>2.0.CO;2).
- Tallapragada, V., Bernardet, L., Biswas, M.K., Gopalakrishnan, S., Kwon, Y., Liu, Q., Marchok, T., Sheinin, D., Tong, M., Trahan, S., Tuleya, R., Yablonsky, R., Zhang, X., 2014. In: Bernardet, L. (Ed.), *Hurricane Weather Research and Forecasting (HWRF) Model: 2014 Scientific Documentation*. NCAR Development Tested Bed Center Report, Boulder, CO 81pp.
- Thompson, P.R., Mitchum, G.T., 2014. Coherent sea level variability on the North Atlantic western boundary. *J. Geophys Res Oceans* 119, 5676–5689. <https://doi.org/10.1002/2014JC009999>.
- Todd, R.E., Asher, T.G., Heiderich, J., Bane, J.M., Luettich, R.A., 2018. Transient response

- of the Gulf stream to multiple hurricanes in 2017. *Geophys. Res. Lett.* 45. <https://doi.org/10.1029/2018GL079180>.
- Tully, K., Gedan, K., Epanchin-Niell, R., Strong, A., Bernhardt, E.S., BenDor, T., Mitchell, M., Kominoski, J., Jordan, T.E., Neubauer, S.C., Weston, N.B., 2019. The invisible flood: the chemistry, ecology, and social implications of coastal saltwater intrusion. *BioScience* 69 (5), 368–378. <https://doi.org/10.1093/biosci/biz027>.
- Valle-Levinson, A., Dutton, A., Martin, J.B., 2017. Spatial and temporal variability of sea level rise hot spots over the eastern United States. *Geophys. Res. Lett.* 44, 7876–7882. <https://doi.org/10.1002/2017GL073926>.
- Wdowinski, S., Bray, R., Kirtman, B.P., Wu, Z., 2016. Increasing flooding hazard in coastal communities due to rising sea level: case study of Miami Beach, Florida. *Ocean Coast Man* 126, 1–8. <https://doi.org/10.1016/j.ocecoaman.2016.03.002>.
- Woodworth, P.L., Maqueda, M.M., Gehrels, W.R., Roussenov, V.M., Williams, R.G., Hughes, C.W., 2016. Variations in the difference between mean sea level measured either side of Cape Hatteras and their relation to the North Atlantic Oscillation. *Clim. Dyn.* 49 (7–8), 2451–2469. <https://doi.org/10.1007/s00382-016-3464-1>.
- Wu, C.R., Chang, Y.L., Oey, L.Y., Chang, C.W.J., Hsin, Y.C., 2008. Air-sea interaction between tropical cyclone Nari and Kuroshio. *Geophys. Res. Lett.* 31, L12605. <https://doi.org/10.1029/2008GL033942>.
- Xue, H., Mellor, G., 1993. Instability of the Gulf Stream front in the South Atlantic Bight. *J Phys Oceanog* 23, 2326–2350. [https://doi.org/10.1175/1520-0485\(1993\)023<2326:IOTGSF>2.0.CO;2](https://doi.org/10.1175/1520-0485(1993)023<2326:IOTGSF>2.0.CO;2).
- Yablonsky, R.M., Ginis, I., Thomas, B., Tallapragada, V., Sheinin, D., Bernardet, L., 2015. Description and analysis of the ocean component of NOAA's operational Hurricane Weather Research and Forecasting (HWRF) Model. *J Atmos Ocean Tech* 32, 144–163. <https://doi.org/10.1175/JTECH-D-14-00063.1>.
- Zegarra, M.A., Schmid, J.P., Palomino, L., Seminario, B., 2020. Impact of Hurricane Dorian in the Bahamas: A View from the Sky. Inter-American Development Bank Publication, Technical Note no IDB-TN-1857. 13pp. IDB, Washington DC, USA.